

Workloop Energetics of Antagonist Muscles

Waleed Farahat and Hugh Herr

Abstract—The capability of muscle to produce mechanical work under periodic motions has been traditionally estimated using the workloop technique. We extend this method by allowing a pair of antagonist muscles to interact against a common load with non-zero admittance. We present an experimental approach to measuring the work done by a two-muscle system and show preliminary data. A complimentary problem is to maximize the work produced by the muscle pair in this setting. We formulate this problem in an optimal control framework. We derive conditions for the optimal activation of muscles to produce the maximum work, and show computed solutions.

I. INTRODUCTION

The capability of muscle to produce mechanical work under periodic motions has been traditionally estimated using the workloop technique. This technique was pioneered by Josephson [1], and has since then been the standard method for estimating the energetics of muscle in different species [2], [3], [4], [5]. In this technique, the mechanical power delivered by the muscles is characterized by imposing sinusoidal motion on a muscle while activating it via electrical stimulation for a brief duration at a particular phase of the cycle. Consequently a contraction force is generated, and a cyclic plot of force versus displacement defines a workloop. The instantaneous mechanical power delivered by the muscle is the product of the force and velocity of the interaction point. Integrating this power over a complete cycle yields an estimate of the work done by the muscle on its load, and is represented by the area enclosed by the workloop.

While the workloop technique provides a benchmark test for estimating power output capability of muscle, it also provides a qualitative description of the function of muscle. In [6], it was shown that the shape, volume, and direction of a workloop provide a succinct description of its function in a periodic setting. For example, muscles can act as motors, breaks, springs, or struts, and thereby achieving different functional tasks.

In this paper, we extend the workloop method in several ways. First, we allow the muscles to operate against loads that admit interaction. By contrast, in [1] and the ensuing literature, motion is imposed on a muscle with zero admittance. Therefore, in our tests, the muscle forces *cause* the motion of the load as would be expected in realistic

situations. Second, we allow for two muscles to interact against a common (virtual) load in an antagonist manner. This allows for testing how muscle co-contraction affects net workloop energetics and power transmission. Third, we provide a mathematical framework that is based on optimal control theory to maximize the work output of a muscle under loading conditions, instead of searching for the optimal parameters empirically.

This problem is of interest for several reasons. First, it provides insight to the energetic interaction of muscles and loads in biomechanical systems. Second, it may provide an energetic interpretation to *in vivo* observations for muscle co-contracting during periodic cyclic motions. Thirdly, maximizing a muscle's mechanical work output may be desirable for certain applications, such as electrically stimulated induced workout (such as cycling) for stroke patients.

It what follows, we present the experimental procedure and show preliminary results. In terms of maximizing muscle power output, we present a mathematical formulation, derivation of the optimal control, and simulation results.

II. EXPERIMENTAL INVESTIGATIONS

A. Methods

Experiments are conducted on *plantaris longus* muscles harvested from leopard frogs (*Rana pipiens*). Adult male frogs (approximately 30-50 grams in weight) were used.

The testing apparatus used for the experiments is fully described in [7]. Briefly, each muscle is placed in amphibian's Ringer's solution. The two ends each muscle are attached to a servo system that imposes a programmed mechanical boundary condition on each muscle. For each muscle, force, and position signals are measured. A real-time feedback servo system is programmed to achieve a desired behavior (e.g. the response of a mass-spring-damper system) via admittance control based on the desired forces.

The two systems are linked together via the real-time control software to provide the effect of antagonist motions. Therefore, if one muscle lengthens as the agonist while the other contracts commensurately as the antagonist. The virtual load "attached" to the two muscles is excited by the net force measured by both muscles as shown in figure 1. Therefore, the two muscles contribute to the excitation of the load while interacting with the same response (with opposing signs). This arrangement allows for muscles to interact *in vitro* while seeing a common load. The load can be programmed easily in servo with different parameters.

Muscles are surgically harvested from the frogs¹. Prior to

¹All experiments are performed according to the guidelines and protocols approved by the MIT Committee on Animal Care.

Waleed Farahat is with the Mechanical Engineering Department, Massachusetts Institute of Technology, Cambridge, MA 02139, USA wfarahat@mit.edu

Hugh Herr is with The Media Laboratory, Harvard-MIT Health Science and Technology Division, Massachusetts Institute of Technology, Cambridge, MA 02139, USA, and also with the Department of Physical Medicine and Rehabilitation, Harvard Medical School, Spaulding Rehabilitation Hospital, Boston, MA 02114, USA hherr@media.mit.edu

removal from the animal, the muscle rest length was measured with both the knee joint and the hip joint positioned at 90 degrees. One end of the muscle is attached to the moving servo (emulating the boundary conditions) while the other is attached to a fixed end (in series with the force sensor). Periodic testing throughout the experiment ensured that there was no slack or slippage of the muscle specimen. Tests included visual inspection as well as monitoring the shape and peak levels of single isometric twitch force profiles. The muscle was submerged in a tub of Ringer's solution that was circulated via a peristaltic pump. The solution was generously oxygenated via direct O₂ gas bubbling at an insertion point in the circulation loop.

Stimulation was delivered through a suction electrode to the sciatic nerve of the muscle. Initial successive isometric twitch measurements were used to establish full recruitment voltage levels, beyond which there was no increase in force production. Additionally, isometric twitch tests were interleaved periodically within experimental measurements to ensure that the muscle did not fatigue, and that force production levels remained constant throughout the duration of the experimental session. When muscle twitch force levels decreased to below 90% of their initial value, the ensuing data were discarded.

The muscles were stimulated via pulse trains, consisting of 8 pulses, 1 ms wide at a frequency of 200 Hz. The trains were delivered at alternating bursts at 4 Hz. The stimulus bursts provided to the agonist were 180° out of phase with those of the antagonist.

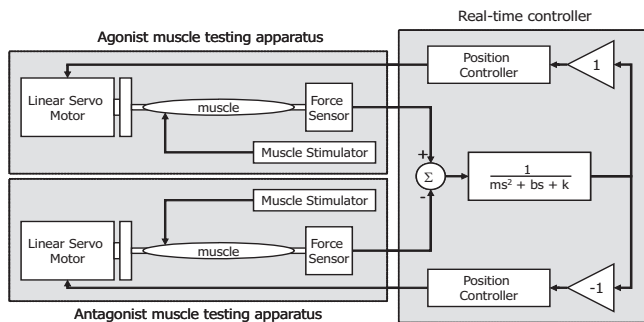


Fig. 1. Block diagram describing experimental setup. Each of the apparatuses controls the motion of a muscle using a linear motor. The forces are measured, subtracted, and filtered with the transfer function of the virtual load. The output is taken as the reference trajectory of motion controllers imposing the motion on the muscles.

B. Results

Initial workloop experimental results are shown in Figure 2. The individual workloops due to each individual muscle are shown, as well as the workloop due to the net overall interaction of the muscles. The plots are shown for a 10 cycles. Note that for successive cycles, the volume of workloops diminishes, primarily due to muscle fatigue. Upon a sufficient rest period, the initial values are typically maintained.

It is observed that the workloops of each individual muscle has two distinct regions. One major sub-loop is more

voluminous, and is due to the active forces developed by each muscle upon stimulation. Other minor sub-loop is due to passive contraction when the opposing muscle is activated and pulls the load. Not surprisingly, the active sub-loop contributed most to the work done on the load.

III. DYNAMICAL ANALYSIS AND OPTIMIZATION

In this section, we pose the question of maximizing the mechanical power output of the muscle-actuated system tested in the experiments above. This problem is cast as an optimal control problem, where the control is the activation of the muscle. The dynamical constraints are the equations of motion of the mass-spring-damper load, as well as the constitutive relations of the muscle.

A. System Dynamics

Consider an antagonist muscle pair acting on a common load as shown in figure 3.

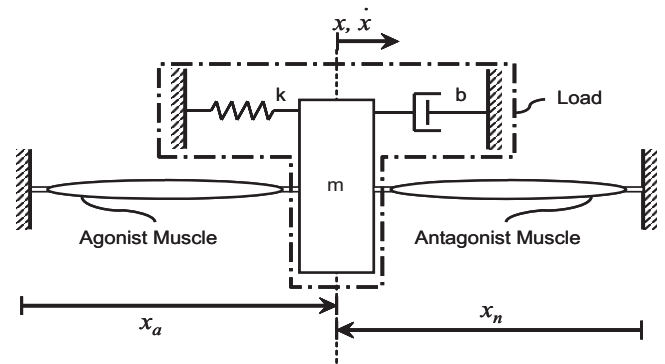


Fig. 3. Antagonist muscle pair acting on a common mass-spring-damper system.

Each muscle is modeled according to the following bilinear model:

$$F_a = A_a + B_a x_a + C_a u_a + D_a x_a u_a + E_a \dot{x}_a + G_a \dot{x}_a u_a$$

$$F_n = A_n + B_n x_n + C_n u_n + D_n x_n u_n + E_n \dot{x}_n + G_n \dot{x}_n u_n$$

where F_i is the muscles contractile forces, the coefficients are A_i through G_i , x and \dot{x} are the position and velocity of the muscles end points, and u is the muscles activation. The subscripts a and n denote agonist and antagonist respectively. The activation u is assumed to be a normalized quantity (ranging between 0 and 1) and is modulated by the stimulus pulse train parameters (such as pulse width, frequency or amplitude).

This formulation, in a very crude sense, captures some of the muscle's basic characteristics. The muscles passive elastic and viscous properties are captured by the coefficients B and E . The active force generated is captured by C . The dependence of stiffness and damping on the muscle's activation is captured by the coefficients D and F . Finally, A represents a residual force. This formulation may also be justified by taking a truncated Taylor's series expansion of muscle force, retaining only linear and first order coupling terms.

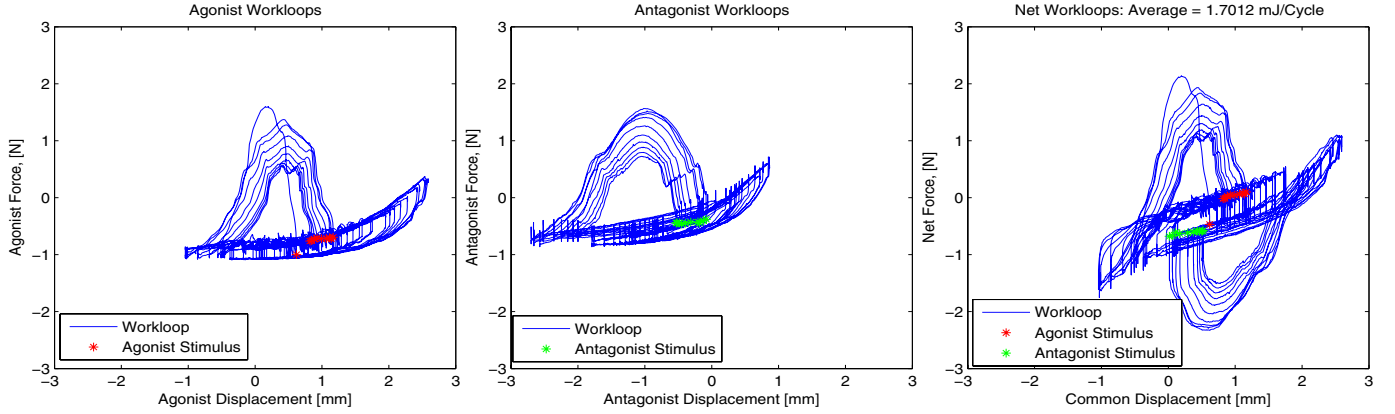


Fig. 2. Experimental workloop data. The muscle forces is plotted against its displacement. The left plot is for the agonist muscle while the center plot is for the antagonist muscle. The right plot is for the entire system with the net force plotted on the y-axis. The points of muscle stimulation are indicated by the asterisks. The area of the workloop indicated the work done by the muscle. Values are indicated on the respective figures.

Define the coordinates $x_a = x + x_a^0$ and $x_n = -x + x_n^0$ as the local coordinates of the muscles, where x is the mass coordinate and x_a^0 and x_n^0 are nominal lengths (as shown in figure 1). Assuming identical muscles (i.e. $A_a = A_n = A$, $B_a = B_n = B$, ...etc, and that $x_a^0 = x_n^0$), we write:

$$\begin{aligned} F_{net} &= F_a - F_n \\ &= 2Bx + C(u_a - u_n) + D(x + x^0)(u_a + u_n) + 2E\dot{x} + G\dot{x}(u_a + u_n) \end{aligned} \quad (1)$$

The net muscle force that acts on the load is given by:

$$F_{net} = m\ddot{x} + b\dot{x} + kx \quad (2)$$

Define the following vector quantities: $\mathbf{x} = [x; \dot{x}]$, $\mathbf{u} = [u_a; u_n]$. Then the dynamics of the system may be compactly written as:

$$\begin{aligned} \dot{\mathbf{x}} &= \begin{bmatrix} 0 & 1 \\ \frac{-k+2B}{m} & \frac{-b+2E}{m} \end{bmatrix} \mathbf{x} + \\ & \begin{bmatrix} 0 & 0 \\ \frac{G\dot{x}+D(x+x^0)+C}{m} & \frac{G\dot{x}+D(x+x^0)-C}{m} \end{bmatrix} \mathbf{u} \\ \dot{\mathbf{x}} &= \mathbf{f}(\mathbf{x}, \mathbf{u}) \end{aligned} \quad (3)$$

Note that this system is nonlinear since the mechanical state variables x and \dot{x} are directly multiplied by the control $[u_a; u_n]$.

B. Maximization of Mechanical Energetic Output

Our objective is to maximize the mechanical energy output by the muscle pair to the load over periodic motions. The following discussion assumes familiarity with optimal control theory (see [8]). The instantaneous power output is $F_{net}\dot{x}$. Therefore the quantity to be maximized is the integral of $F_{net}\dot{x}$. Alternatively, we may minimize $-F_{net}\dot{x}$.

$$J = \min_{\mathbf{u}} \int_0^T -F_{net}\dot{x}dt = \min_{\mathbf{u}} \int_0^T L(\mathbf{x}, \mathbf{u})d\mathbf{t}$$

$$\begin{aligned} \text{s.t.} \quad \dot{\mathbf{x}} &= \mathbf{f}(\mathbf{x}, \mathbf{u}) \\ 0 &\leq u_i \leq 1 \quad i \in \{a, n\} \end{aligned}$$

The Hamiltonian is a scalar function $H(\mathbf{x}, \mathbf{u})$ and is given by:

$$\begin{aligned} H(\mathbf{x}, \mathbf{u}) &= L(\mathbf{x}, \mathbf{u}) + \lambda^T \mathbf{f}(\mathbf{x}, \mathbf{u}) \\ &= \dot{x}(-2Bx - 2E\dot{x} + (G\dot{x} + D(x + x^0) + C)u_a + (G\dot{x} + D(x + x^0) - C)u_n) + \\ & \lambda^T \begin{bmatrix} 0 & 1 \\ \frac{-k+2B}{m} & \frac{-b+2E}{m} \end{bmatrix} \mathbf{x} + \\ & \lambda^T \begin{bmatrix} 0 & 0 \\ \frac{G\dot{x}+D(x+x^0)+C}{m} & \frac{G\dot{x}+D(x+x^0)-C}{m} \end{bmatrix} \mathbf{u} \end{aligned} \quad (4)$$

where λ is a 2×1 vector of Lagrange multipliers. From the Pontryagin minimum principle [8], under conditions of optimal control trajectories, the evolution of the co-state variables are governed by:

$$\dot{\lambda}^T = -\frac{\partial H}{\partial \mathbf{x}} = -\frac{\partial L}{\partial \mathbf{x}} - \lambda^T \frac{\partial \mathbf{f}}{\partial \mathbf{x}} \quad (5)$$

Equations 3 and 5 define a two-point boundary value problem with boundary conditions defined by:

$$\mathbf{x}(t=0) = \mathbf{x}_0; \quad \lambda(t=T) = \mathbf{0}$$

The optimal control u^* is characterized by

$$u^* = \arg \min_{\mathbf{u}} H(\mathbf{x}, \mathbf{u}) \quad (6)$$

Since the Hamiltonian is linear in the control (as per equation

5), the following switching functions are used:

$$u_a^* = \begin{cases} 1 & \text{if } (G\dot{x} + D(x+x^0) + C)(\lambda_2/m - \dot{x}) > 0 \\ 0 & \text{if } (G\dot{x} + D(x+x^0) + C)(\lambda_2/m - \dot{x}) \leq 0 \end{cases} \quad (7)$$

$$u_n^* = \begin{cases} 1 & \text{if } (G\dot{x} + D(x+x^0) - C)(\lambda_2/m - \dot{x}) > 0 \\ 0 & \text{if } (G\dot{x} + D(x+x^0) - C)(\lambda_2/m - \dot{x}) \leq 0 \end{cases} \quad (8)$$

From the analysis above, and for the muscle model utilized, we recognize that this is a bang-bang control problem, with the optimal control u_a^* and u_n^* being determined according to the sign of the switching expressions $(F\dot{x} + D(x+x^0) + C)(\lambda_2/m - \dot{x})$ and $(F\dot{x} + D(x+x^0) - C)(\lambda_2/m - \dot{x})$ respectively. This results in a discontinuous control law.

C. Solution of the Optimal Control Problem

The solution of the optimal control problem relies on the solution of the two-point boundary value problem characterized by the dynamical equations 3, 5 and the control law 6, with initial conditions 6. This problem is solved using the function `bvp4c` in `MATLAB`. This function implements the finite difference collocation algorithm given in [9]. The solver uses a collocation approach approximating the solution by piece-wise cubic polynomials. The residuals and the boundary conditions are minimized using a nonlinear search scheme. In order for the solution to be attained without running into Jacobian singularities, the control function is smoothed. Successive iterations of the solution increase the sharpness of the smoothing function, with the solution of one iteration used as the initial guess for the solution of the following iteration.

D. Simulation Results

We define the problem in terms of normalized parameters as follows: $A = 0$, $B = 100$ passive stiffness, $C = F_{max} = 5$ maximum isometric active force, $D = F_{max}/l_o = 5/0.025 = 40$, $E = 5$ passive muscle damping, $G = 1$ active muscle damping. The mass-spring-damper system was chosen with a natural frequency of 3 Hz and a damping ratio of $\zeta = 0.15$. The result of the bang-bang optimal control solution is shown in figure 4.

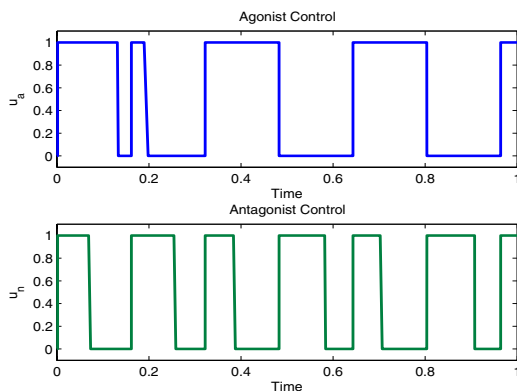


Fig. 4. Optimal control time histories. Notice the bang-bang control profile.

IV. DISCUSSION

This paper presents preliminary experimental and analytical results towards understanding the energetics of antagonist muscles pairs. The two approaches are complimentary.

While the left and right *plantaris longus* muscles used do not play the roles of antagonist pairs in frogs, we had them play that role *in vitro* in the experimental setup employed. The main reason for this was to extract two muscles that are as closely identical as possible in order to simplify the interpretation of the results. We notice that from figure 2 the individual workloops are largely similar and of comparable magnitudes.

On the optimal control side, we notice that the optimal solution computed stimulates the muscles via periodic cycles at the natural frequency of the modeled mass-spring-damper system. This is expected since this is the frequency of maximal power output. We also notice that some degree of co-contraction is observed. We hypothesize that this co-contraction is beneficial to enhance the net workloop energetics and the transmission of power to the load.

Future work includes understanding the effect of muscle co-contraction on the energetics of muscle pairs, and questioning experimentally verifying if there are certain situations in which co-contraction is favorable from an energetics point of view. Future work also includes developing a more systematic approach towards spanning a larger space of stimulation parameters, and correlating between experimental muscle work output results and the solutions of the optimal control problem. Additionally, the framework presented may be extended to more comprehensive muscle models that take into account recruitment and activation dynamics. Finally, it would be interesting to employ identification methods to estimate the coefficients of the muscle model.

REFERENCES

- [1] Robert Josephson. Mechanical power output from striated muscle during cyclic contraction. *J. Exp. Biol.*, 114:493–512, 1985.
- [2] E. Don Stevens. The pattern of stimulation influences the amount of oscillatory work done by frog muscle. *Journal of Physiology*, 494(1):279–285, 1996.
- [3] E. Luiker and E. Don Stevens. Effect of stimulus train duration and cycle frequency on the capacity to do work in the pectoral fin of muscle of the pumpkinseed sunfish, *Lepomis gibbosus*. *Can. J. of Zool.*, 71:2185–2189, 1993.
- [4] Darrell Stokes and Robert Josephson. The mechanical power output of a crab respiratory muscle. *J. Exp. Biol.*, 140:287–299, 1988.
- [5] Anna Ahn and Robert Full. A motor and a brake: Two leg extensor muscles acting at the same joint manage energy differently in a running insect. *J. Exp. Biol.*, 205:379–389, 2002.
- [6] Michael H. Dickinson, Claire T. Farley, Robert J. Full, M. A. R. Koehl, Rodger Kram, and Steven Lehman. How animals move: An integrative view. *Science*, 288(2):100–106, 2000.
- [7] Waleed Farahat and Hugh Herr. An apparatus for characterization and control of isolated muscle. *IEEE Trans. Neural Syst. Rehab. Eng.*, 13(4):473–481, December 2005.
- [8] Arthur E. Bryson and Yu-Chi Ho. *Applied Optimal Control: Optimization, Estimation and Control*. John Wiley & Sons, New York, 1975.
- [9] Lawrence F. Shampine and Jacek Kierzenka. Solving boundary value problems for ordinary differential equations in `MATLAB` using `bvp4c`. 2000.